180° Positron-Electron Scattering at 200 and 500 MeV

A. BROWMAN,* B. GROSSETÊTE, AND D. YOUNT†
Ecole Normale Supérieure, Laboratoire de l'Accélérateur Linéaire, 91 Orsay, France
(Received 10 June 1966)

To test the predictions of quantum electrodynamics, absolute and relative measurements of the positron-electron scattering cross section were made at 200 and at 500 MeV. Recoil electrons were detected with the spectrometer at 0° with respect to the incident-beam direction, and for the range of recoil momenta studied, the elastic-scattering cone was entirely contained in the angular acceptance of the spectrometer. This method permitted high precision and an experimental test of the radiative corrections. The absolute accuracy of the cross sections was 1%. The complete radiative corrections for this experiment are not yet available. However, for purposes of orientation, one may extrapolate existing calculations to the present situation. If one does this, the shape of the recoil spectrum near the incident positron momentum is consistent with the theory if the radiative corrections of the form $1+\epsilon$ are used (χ^2 probability of 0.5); the shape is in less good agreement if the correction has the form e^δ (χ^2 probability of 0.2). The most precise measurements made, where the corrections were about 15%, were in agreement with the theory. The accuracy has to be increased to decide between e^δ and $1+\delta$. If radiative corrections are assumed to be precisely known, the experiment determines $1/K$ to about 0.6 F, where a violation of quantum electrodynamics of the form $\sigma\rightarrow\sigma_0(1-q^2/K^2)^2$ is assumed, and where σ is the quantum-electrodynamical cross section and q is the four-momentum transfer. A significant increase in sensitivity could be achieved by extending the experiment to available positron energies well above the relatively modest values used here.

I. INTRODUCTION

In high-energy electron-electron or positron-electron scattering experiments the four-momentum transfer is proportional to the square root of the incident energy when the target electron is at rest, while it is proportional to the sum of the energies when the two particles collide in the center-of-mass system. Since deviations from quantum electrodynamics (QED),[1] due possibly to a finite electron-charge distribution or to breakdown of Coulomb's law at short distances, are expected to depend upon the four-momentum transfer, it is generally assumed[2] that clashing-beam experiments will far surpass anything that can be done in the laboratory system. In spite of its considerable advantage, we have been impressed by the difficulties and expense inherent in the clashing-beam approach. We have therefore posed the question: To what extent can one substitute high precision in the laboratory system for the high momentum transfer obtainable in the center-of-mass system?

In discussions of possible violations of QED, the expression

$$\sigma\rightarrow\sigma_0(1-q^2/K^2)^2 \tag{1}$$

is frequently assumed,[1,3] where σ_0 is the unviolated electrodynamic cross section, σ the violated cross section, $q^2>0$ the squared four-momentum transfer, and K a constant. Assuming $(q^2/K^2)\ll 1$, the constant K can be associated, by the relation

$$1/K^2\approx\langle r_e\rangle^2 2/3\hbar^2+1/\hbar^2\Lambda^2, \tag{2}$$

with a rms radius $\langle r_e\rangle$ leading to an electron form factor $F_e(q^2)\approx(1-\langle r_e\rangle^2 q^2/6\hbar^2)$, and with an altered Coulomb potential $1/r\rightarrow(1/r)[1-e^{-\Lambda r}]$ resulting in an altered photon propagator $-1/q^2\rightarrow(-1/q^2)(1-q^2/\hbar^2\Lambda^2)$.

For incident electrons or positrons of energy $E_{\rm lab}$ and rest mass mc^2, the four-momentum transfer in a scattering through laboratory angle $\theta_{\rm lab}$ is

$$q=[(2E_{\rm lab}/c)\sin\theta_{\rm lab}/2]/[1+2(E_{\rm lab}/mc^2)\sin^2\theta_{\rm lab}/2]^{1/2}\leq(2mE_{\rm lab})^{1/2}, \tag{3}$$

while for two particles each having center-of-mass (c.m.) energy $E_{\rm c.m.}$, the four-momentum transfer is

$$q=(2E_{\rm c.m.}/c)\sin\theta_{\rm c.m.}/2\leq 2E_{\rm c.m.}/c. \tag{4}$$

Thus for laboratory and center-of-mass experiments on positron-electron scattering at 180°, the ratio R of the deviations for a given k^2 is

$$R=(q^2)_{\rm lab}/(q^2)_{\rm c.m.}=2mE_{\rm lab}/(2E_{\rm c.m.}/c)^2. \tag{5}$$

Assuming $E_{\rm lab}=E_{\rm c.m.}=500$ MeV, a "precision factor" of about 1/2000 results; while for $E_{\rm lab}=20$ GeV and $E_{\rm c.m.}=500$ MeV, the factor is 1/50.[4] Although the present experiment is an order of magnitude more sensitive than previous experiments on either positron-electron[5] or electron-electron[6] scattering, because of its

* Present address: Department of Physics, Cornell University, Ithaca, New York.

† National Science Foundation Postdoctoral Fellow; now at Stanford Linear Accelerator Center, Stanford University, Stanford, California.

[1] S. D. Drell, Ann. Phys. (N. Y.) 4, 75 (1958).

[2] W. C. Barber, B. Richter, W. K. H. Panofsky, G. K. O'Neill, and B. Gittelman, Hansen Laboratory Report No. HEPL-170, Stanford, California, 1959 (unpublished).

[3] Yung-Su Tsai, in *Proceedings of the 1960 Annual International Conference on High Energy Physics at Rochester* (Interscience Publishers, Inc., New York, 1960), p. 771.

[4] In electron-electron experiments the maximum momentum transfer occurs at $\theta_{\rm c.m.}=90°$, giving the 180° positron experiments an advantage of $\sin^2(180/2)/\sin^2(90/2)=2$. However, see V. N. Bayer and S. A. Kheifets, Nucl. Phys. 47, 313 (1963), where it is shown that under certain assumptions, the maximum deviation from QED for both electron and positron experiments occurs at 90° c.m. scattering angle.

[5] J. A. Poirier, D. M. Bernstein, and Jerome Pine, Phys. Rev. 117, 557 (1960).

[6] E. B. Dally, Phys. Rev. 123, 1840 (1961).

low momentum transfer, it cannot compete with clashing-beam experiments now in progress.[2,7,8] We believe, however, that the method is directly applicable at energies up to 20 GeV and that it would lead to comparable precision at these energies. Such an experiment would compare favorably with the clashing-beam experiments envisioned for the near future.

The method used here took advantage of the opposite charges of the incident and target particles. A magnetic spectrometer was set at 0° with respect to the incident positron beam direction and was used to detect the recoil electrons while the incident positrons were deflected into the magnet iron. For electrons having nearly the same momentum as the incident positrons, the recoil angle in the laboratory was quite small, and there was a considerable range of momenta over which all of the emerging electrons were within the angular acceptance of the spectrometer. The effective angular acceptance was thus 4π sr, and the counting rate was determined only by the momentum acceptance of the spectrometer and the momenta of the incident positron and recoil electron.

The positron-electron scattering cross section,[9] derived in the first Born approximation, may be written[5]

$$d\sigma_B = d\sigma_R(D+I+A), \tag{6}$$

where $d\sigma_R$ is the classical Rutherford cross section and where the terms D, A, and I are due, respectively, to direct scattering from the charge and Dirac magnetic moment, to virtual annihilation, and to the interference between these terms. For highly relativistic incident positrons the cross section has the simple form

$$d\sigma_B = 0.499\times10^{-24}(mc^2/E_+)(d\epsilon/\epsilon^2)(1-\epsilon+\epsilon^2)^2 \text{ cm}^2, \tag{7}$$

where $\epsilon=(E_- - mc^2)/(E_+ - mc^2)$ and E_+ and E_- are the total energies of the incident positron and recoil electron. This relativistic approximation differs from the exact formula by less than 0.2% in our energy range.

If $0.9E_+<E_-<E_+$ one can make the qualitative approximations $\epsilon\approx E_-/E_+$, $E_-\approx E_+$, thus obtaining

$$d\sigma_B \approx 0.5\times10^{-24}(mc^2/E_+)(dE_-/E_+) \text{ cm}^2. \tag{8}$$

For a fixed spectrometer resolution, $\Delta p_-/p_- \approx dE_-/E_- \approx dE_-/E_+$, the cross section varies only as $1/E_+$ and is rather constant as a function of the spectrometer setting $p_- \approx E_-/c$.

The electrodynamic cross section is severely modified when p_- is within 1–2% of p_+, since the radiative corrections approach 100% as p_- approaches p_+. This behavior is predicted by Meister and Yennie[10,11] in the formula

$$\delta \cong \frac{\alpha}{\pi}\left\{\left[\ln\left(\frac{2E_1E_4}{mc^2E_3}\right)-1\right]\ln\left(\frac{E_1^2}{E_3E_4}r^3\right)-\tfrac{1}{2}\ln^2\left(\frac{E_3}{E_4}r\right) + \frac{11}{3}\ln\left(\frac{2E_4}{mc^2}\right)-\tfrac{3}{4}\ln\left(\frac{E_1}{mc^2}r\right)\right\}, \tag{9}$$

where in their notation E_1 and E_3 are the initial and final positron energies, E_4 is the final electron energy, and r depends upon the conditions of the experiment. Meister and Yennie conjecture that "if δ' is the doubly logarithmic part of δ, the expression

$$e^{\delta'}(1+\delta-\delta') \tag{10}$$

yields a better estimate of the radiative corrections than does the original estimate $(1+\delta)$." This is a refinement of the exponentiation $\sigma=\sigma_0 e^{\delta}$, originally conjectured by Schwinger[12] and shown to be valid for the infrared contributions by Yennie and Suura.[13] For this experiment the two types of exponentiation give the same result to within 0.1% of the corrected cross section in the region $E_-<0.995E_+$, and they differ by less than 0.5% over the entire recoil-electron spectrum. Furthermore, the correction is dominated by the infrared term [i.e., by the first doubly logarithmic term in Eq. (9)] in the region near E_+, and it is only in this region that the difference between e^{δ} and $(1+\delta)$ is large.

After the radiative corrections have been made, the shape of the electron spectrum, expressed as the rate versus the percent down from p_+, is essentially independent of p_+. In addition there remains a substantial range over which the cross section is relatively constant as a function of p_-. In this region uncertainties in p_- are not important, and the counting rate for a given $\Delta p_-/p_-$ is easily calculated. Since q^2 is also fairly constant over this range, the shape of the electron spectrum is not expected to be sensitive to violations of QED.

It is kinematically impossible for radiation to occur during the scattering process in such a way that a recoil electron of momentum p_- will be outside of the elastic-scattering cone appropriate for this momentum. The radiative corrections were thus determined by $E_1=p_+c$ and $E_4=p_-c$, and the parameter r in Eq. (9) was given for this experiment by[14]

$$r=(1-E_4/E_1). \tag{11}$$

Since p_+ and p_- were accurately known and since the corrections were independent of the spectrometer angular acceptance, so long as this acceptance included the

[7] F. Amman *et al.*, in *Proceedings of the International Conference on High Energy Accelerators, Dubna, 1963* (Atomizdat, Moscow, 1964), p. 249.

[8] A. Blanc-Lapierre *et al.*, in *Proceedings of the International Conference on High Energy Accelerators, Dubna, 1963* (Atomizdat, Moscow, 1964), p. 288.

[9] H. J. Bhabha, Proc. Roy. Soc. (London) **A154**, 195 (1936).

[10] N. Meister and D. R. Yennie, Phys. Rev. **130**, 1210 (1963).

[11] The Meister and Yennie calculation of δ omits some terms ("internal radiative corrections"), which may be of importance in this experimental region. A more exact calculation is in progress. D. R. Yennie and R. K. Kuo (private communication).

[12] J. Schwinger, Phys. Rev. **76**, 790 (1949).

[13] D. R. Yennie and H. Suura, Phys. Rev. **105**, 1378 (1957).

[14] This expression for r differs from the formula of Meister and Yennie (4.6 b) by a factor of 2 due to the fact that $\Delta\theta=\theta_4$ is not small compared to θ_4. D. R. Yennie (private communication).

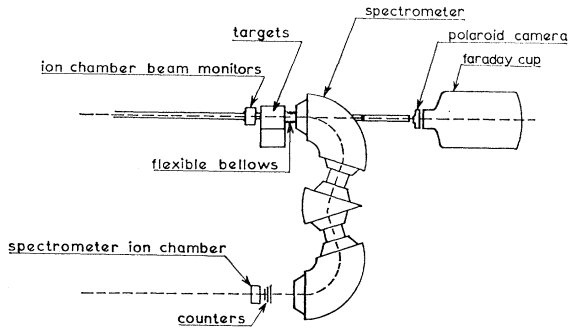

FIG. 1. Experimental setup in vertical section. Momentum-analyzed positrons entered from the left and were incident on the ion-chamber beam monitors and various other targets. Recoil electrons from positron-electron scattering were momentum-analyzed by the three-magnet spectrometer set at 0° and were detected by scintillation counters at the focus of the spectrometer. The Polaroid camera, Faraday cup, and spectrometer ion chamber were used in various tests described in the text. The accelerator vacuum extended to the entrance window of the ion chamber while the spectrometer vacuum chamber extended from the exit window to within a half meter of the Faraday cup and the counters.

elastic-scattering cone, the uncertainties in the calculated radiative corrections were theoretical in nature. We regarded these corrections as being part of the electrodynamic process under investigation and not as an effect leading to experimental errors.

The procedure was to use a narrow momentum resolution to study the radiative corrections, concentrating on the region near p_+, and to test QED by measuring the cross sections at different p_+, using a wider resolution and a momentum setting on the flat portion of the spectrum a fixed percent down from p_+. The wider setting was preferable at the data points since $\Delta p_-/p_-$ had to be determined experimentally at these points. The invariant shape and flatness of the spectrum and the $1/p_+$ dependence of the cross section were among the factors which permitted a high-precision experiment.

II. APPARATUS

Figure 1 shows the experimental set up in vertical section. Momentum-analyzed positrons[15] from the Orsay linear accelerator passed through thin ionization-chamber monitors and were incident on various targets located at the center of rotation of the double-focusing, zero-dispersion spectrometer.[16] The recoil electrons were momentum-analyzed with the spectrometer set at 0° and were detected by scintillation counters. Another ion chamber placed just in back of the counters was used in studies of the spectrometer momentum and angular acceptance. The scattering chamber surrounding the targets was connected directly to the vacuum chamber of the spectrometer and extended to the exit window of the ion chamber. The accelerator vacuum extended to the entrance window. Flexible bellows were used between the scattering chamber and the spectrometer to permit changes in the spectrometer angle of about $\pm 2°$.

The three-magnet deviation system[16] used to momentum-analyze the incident beam was calibrated by a floating-wire measurement[16,17] believed to be accurate to a few parts in 10^3. The field in the first analyzing magnet was monitored during the runs with an NMR probe. The momentum slits for positrons were set at $\Delta p/p = 0.5\%$ or 1.0%, and the collimator settings varied from 5 mm×5 mm to 15 mm×15 mm, depending on the measurements being made. The momentum acceptance of the spectrometer was measured with incident electrons analyzed with $\Delta p/p = 0.25\%$ and a 2-mm×2-mm collimator.

The beam monitors consisted of three thin-walled, hydrogen-filled ion chambers having sensitive volumes defined by parallel aluminum plates oriented perpendicular to the beam direction. Two of these chambers were used to monitor the beam intensity, while the third, a split-plate chamber similar to that described previously,[18] was used as a beam-position indicator. To minimize the number of entrance and exit windows, the three monitors were enclosed in a single, gas-tight container filled with hydrogen at slightly above atmospheric pressure. The two ion chambers which monitored beam intensity had different thicknesses and thus different saturation characteristics.[18] This provided a check to ensure that at all times at least one of the monitors was being used at beam-current densities so low that saturation was not a problem. The beams were centered at the target to about ± 1 mm with the aid of the beam-position indicator. Beam sizes and positions were checked with Polaroid film placed downstream of the spectrometer where an output port permitted the passage of the beam when the spectrometer field was off. Since the quadrupoles of the analyzing system were not used, the incident beams were highly parallel (angular divergence less than 10^{-3} rad),[16] and the beam spots were rectangular with horizontal and vertical dimensions approximating the collimator settings.

The "1-GeV" Orsay Faraday cup[19] was used to calibrate the ion-chamber beam monitors. Our estimates of the efficiency of this cup are based upon tests described in Ref. 18, as well as upon certain measurements made during the course of this and other positron experiments using the Orsay cup. Independent tests made of "the modified 300-MeV" Stanford cup indicated that the difference in efficiency for positrons and electrons was $(0.00\pm 0.30)\%$ and that the absolute efficiency was therefore $(100.00\pm 0.15)\%$ for both. Measurements of the relative efficiencies of hydrogen ion chambers and

[15] R. Hirel, L. Burnod, and J. Delouya, Rapport Interne LAL-28, 1962 (unpublished).
[16] B. Milman, L'Onde Elec. 42, 310 (1962).
[17] C. Bazin, J. Dupin, and N. K. Loï, Rapport Interne 61-1, 1965 (unpublished).
[18] D. Yount and J. Pine, Phys. Rev. 128, 1842 (1962).
[19] This Faraday cup is similar in design to the "500-MeV" Orsay Faraday cup described by D. Isabelle, L'Onde Elec. 42, 354 (1962).

the Stanford cup for positrons and electrons gave $(0.02\pm0.22)\%$, indicating that at 300 MeV the ionization of hydrogen is the same for electrons and positrons to $\pm0.27\%$. The relative efficiencies measured at Orsay differed by $(0.44\pm0.20)\%$, the apparent efficiency of the Faraday cup being greater for positrons than for electrons. After considering the various factors[18] which could lead to such a difference, we believe that the most probable was the emission of secondary electrons from the Faraday cup. This would amount to $\frac{1}{2}(0.44-0.02)\% = 0.21\%$ of the incident intensity and could possibly be explained by the non-re-entrant geometry of the Orsay cup. Combining the various uncertainties, the estimated efficiency of the Orsay Faraday cup was $(100.21\pm0.20)\%$ for positrons and $(99.79\pm0.20)\%$ for electrons. A $\pm0.20\%$ absolute uncertainty in the value of the integrator capacitors and a $\pm0.15\%$ uncertainty in the ion-chamber calibrations resulted in an absolute uncertainty of $\pm0.34\%$ in the efficiency of the calibrated ion chambers.

The relative efficiency of the ion chambers at 200 and 500 MeV was determined by intercalibrating the ion chambers and Faraday cup at 200, 500, and 850 MeV. Previous tests[18] at the same energies had indicated that the ionization of hydrogen at 1 atm increases by $(+0.37\pm0.08)\%$ over this range, while for 2 atm it changes by $(-0.03\pm0.11)\%$. The present intercalibrations at 1 atm gave a $(+0.15\pm0.15)\%$ "density effect" in agreement with the Stanford results. This suggested that the efficiency of the Orsay cup was constant to $\pm0.15\%$ in the range from 200 to 850 MeV. The difference in the ion-chamber efficiencies at 200 and 500 MeV was taken to be 0.15%, while the relative error appropriate in comparing results at the two energies was 0.10% (i.e., $\pm0.07\%$ at each energy). This does not include the uncertainties due to fluctuations of order 0.1% observed in individual integrations.

Six different targets were used. The first, with a thickness of 0.0023 radiation lengths, consisted of the aluminum and hydrogen of the beam monitors located 55 cm upstream of the center of rotation of the spectrometer. Three polyethylene "data" targets of 0.0025, 0.0046, and 0.0071 radiation lengths (1-, 2-, and 3-mm thickness) and a bismuth target of 0.0181 radiation lengths could be added at the center of rotation. A final polyethylene target of 0.0046 radiation lengths was placed 10 cm upstream and was used only at 500 MeV. The fact that some of the targets were not at the center of rotation of the spectrometer was expected to have negligible effect in this geometry, and no difference was found in the cross sections measured with the targets at different positions. The uniform regions of the movable targets exceeded 4 cm in diameter, while the effective diameter of the beam monitor was 10 cm. The data targets and bismuth targets were mounted in a polyethylene target holder of 0.0046 radiation lengths as a precaution against any enhancement of the scattering which might have occurred if a very small fraction of the beam had been incident on a thick target holder.

TABLE I. Number of electrons per cm² in the different targets. The errors shown are the absolute uncertainties. For all targets except the aluminum, the electrons in the aluminum must be added to the electrons in that target in order to obtain the total number of electrons per cm² in the beam.

Target	Number of electrons (10^{23} cm^{-2})
"Aluminum"	(0.1635 ± 0.0007)
1 mm CH_2	$(0.3531+0.0011)$
2 mm CH_2	(0.6683 ± 0.0020)
3 mm CH_2	(1.0355 ± 0.0031)
2 mm CH_2 (upstream)	(0.6761 ± 0.0020)
Bismuth	(0.2839 ± 0.0009)

After the run, all of the targets except the bismuth target were sacrificed, and central disks 2.000 cm in diameter were punched out and weighed to determine the number of electrons in the path of the beam. The measured weight per unit area of the polyethylene targets was shown to be independent of the size of the punch, provided that punch diameters of 2 cm and larger were used.

Analysis of polyethylene samples from the same sheets from which the targets were cut indicated 1.99 ±0.02 parts of hydrogen per 1 part carbon. This led to a 0.3% absolute uncertainty in the number of electrons in these targets. The uncertainty in the number of electrons per cm² in the bismuth target was also $\pm0.3\%$, while the number of electrons in the beam monitor was known to $\pm0.4\%$. Relative errors in target thickness were $\pm0.2\%$ for the "aluminum" and $\pm0.1\%$ for each of the others. The number of electrons per cm² in the various targets is given in Table I.

The "empty target" background, due to electrons in the beam or to positrons stopping in the magnet iron of the spectrometer, was found to be negligible at both 200 and 500 MeV in a preliminary run with no material in the beam. The beam was held steady and monitored indirectly by counting electrons for fixed periods with and without a known target thickness in the beam. Since the backgrounds were negligible, the beam monitors could be used as a target thus eliminating the statistical errors that would have been present if a subtraction had been necessary.

Studies of the angular acceptance of the spectrometer have been made by Dupin[20] for various momenta spanning the range used here. These studies showed that the vertical acceptance projected into a plane at the entrance of the spectrometer was about 5 times the horizontal acceptance. Thus losses first occurred when, for a fixed p_+, p_- was decreased until the elastic-scattering cone increased beyond the horizontal acceptance or until multiple scattering caused some of the particles to be outside of the acceptance. The range of momenta

[20] J. Dupin, Rapport Interne LAL-1145, 1965 (unpublished).

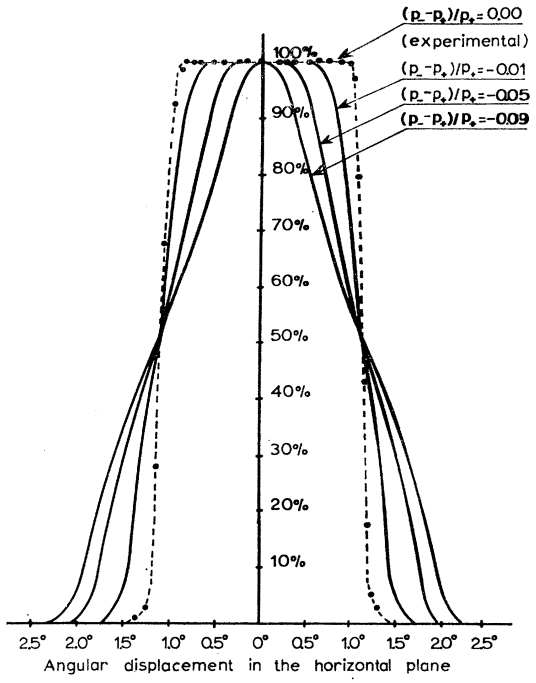

FIG. 2. Angular acceptance of the spectrometer in the horizontal plane at 500 MeV/c. The experimental points joined by the dashed curve indicate the fraction of the incident positron beam transmitted by the spectrometer as a function of the angular setting. This also corresponds to the transmission for electrons from positron-electron scattering with $(p_- - p_+)/p_+ = 0.00$. Theoretical curves for $(p_- - p_+)/p_+ = -0.01$, -0.05, and -0.09 are also shown to indicate how the losses due to multiple scattering and Bhabha scattering become important when p_- decreases with a given p_+.

over which the experiment could be performed was limited mainly by multiple-scattering losses below 200 MeV and by the rapidly decreasing angular acceptance above 500 MeV.

We remeasured the horizontal acceptance at both 200 and 500 MeV by rotating the spectrometer through an angular range of about $\pm 2°$, centered about 0°. For these measurements the spectrometer was set for positrons at the incident beam momentum and the transmitted particles were detected with the spectrometer ion chamber. The measured horizontal acceptances were well centered on the beam line and agreed to within 5% with those obtained by Dupin; the rising portions of the transmission curves provided an excellent measure of the beam spot distribution in the horizontal plane. The results obtained at 500 MeV, normalized to unity, are shown in Fig. 2. Also shown are the curves predicted for the thickest polyethylene target and for various values of p_- when the spectrometer was set to detect the electrons from positron-electron scattering.

The spectrometer with its shunt was calibrated with a floating-wire measurement[20] believed to be accurate to a few parts in 10^3. Since the short-term regulation of the spectrometer was generally better than the reading accuracy of the digital voltmeter used to monitor the shunt voltage, this shunt calibration was transferred to a Hall probe in a series of intercalibrations in which the ratio of the two monitors was measured at about 40 points beginning at a setting of around 600 MeV/c, where the iron is saturated, and decreasing monotonically to about 50 MeV/c. A least-squares fit to the results permitted us to use the more sensitive readings of the Hall probe directly. The ratio of the spectrometer shunt to Hall probe readings was reproducible on different intercalibrations to about 0.1% in the range from 200 to 600 MeV/c. This uncertainty was reflected in p_-. On a given intercalibration run, the difference between two nearby momentum settings could be determined to about 0.01% of p_-, depending upon the short-term regulation of the spectrometer and beam-analyzing magnets. This latter led to errors in $\Delta p_-/p_-$ of about 0.5% when $\Delta p_-/p_-$ was 2%. The results obtained for p_- and $\Delta p_-/p_-$ are described in detail in Sec. III.

The recoil electrons were detected in a two-counter telescope located at the focus of the spectrometer. A third counter, smaller than the telescope counters but larger than the region defined by the transmitted particles, was installed between the two telescope counters. The counters were well shielded, conservatively operated, and no trouble was observed from backgrounds or noise. The ratio of doubles to singles was about 0.99. The ratios of triples over doubles in the first and second counters and triples over doubles in the first and third counters provided a measurement of the bremsstrahlung losses of a few tenths of a percent which occurred in the counters.

The data obtained from the twofold coincidence were recorded by scalers with resolving times smaller than 10 nsec, 50 nsec, and also by scalers with resolving times greater than the beam pulse width. The beam pulse width was monitored continuously during the experiment and was typically 500 nsec. Counting rate corrections were of order 1% or less, and the agreement between different scalers indicated that this correction could be made to about 20% accuracy, corresponding to an uncertainty of about 0.2% in the counting rates.

III. DATA, CORRECTIONS, AND UNCERTAINTIES

The data and the principal corrections and uncertainties are summarized in the tables which follow. Included are a high-resolution study of the recoil-electron spectrum at 500 MeV made with the 3-mm polyethylene target (Table II); low-resolution spectrum studies at 500 (Table III) and 200 MeV (Table IV) made with the 3-mm polyethylene target and with the aluminum and bismuth targets; and low-resolution "data" points obtained with p_- approximately 3% below p_+ for each of the six targets.[21] (Table V).

[21] The high-resolution points were taken with $\Delta p_+/p_+ = 0.5\%$, $\Delta p_-/p_- = 0.471\%$, and a 15-mm×15-mm collimator, while the low-resolution points were taken with $\Delta p_+/p_+ = 0.5$ or 1.0%, $\Delta p_-/p_- = 2.20\%$, and a 7-mm×7-mm collimator.

The high-resolution spectrum was taken to test the radiative corrections. The low-resolution spectra were useful in determining the proper settings for the data points and in testing various corrections and errors. Bismuth was chosen as one of the targets in order to maximize these corrections and to expose any Z-dependent effects which might have been overlooked. Experimental parameters for the data points were chosen in such a way as to minimize the systematic errors.

The first two columns of the data tables identify the points taken. The target is indicated in column 1 and the electron momentum expressed as a percent down from p_+ in column 2. Corrections and errors which changed significantly from point to point are included separately in the tables, while the remaining corrections and errors are shown in the columns labeled δ_{misc} and ϵ_{misc}. All the corrections (δ_i) and the errors (ϵ_i) are expressed as a percent of the final corrected cross section.

"Multiple-scattering" corrections (δ_{ms}) were computed by folding together at each point a Gaussian multiple-scattering distribution, the measured beam-spot distribution, the Bhabha scattering angle for the given p_+ and p_-, and the spectrometer angular acceptance. The spectrometer angular acceptance was approximated by a rectangle with the measured width and infinite height. The error (ϵ_{ms}) was taken to be the larger of 10% of the correction and the error arising from the ± 1 mm uncertainty in the beam-spot position and the uncertainty in the spectrometer acceptance. Since multiple scattering was much more important at 200 than at 500 MeV, no distinction was made between relative and absolute errors.

Corrections for bremsstrahlung followed by pair production (δ_{pp}) or by Compton scattering (δ_{Compton}) were evaluated by folding together the Bethe-Heitler[22] formula and the formulas given by Rossi.[23] Corrections for trident production (δ_{tri}) were calculated from formulas given by Murota, Ueda, and Tanaka.[24] In each case, we have assumed that all of the electrons produced in the proper momentum interval were within the angular acceptance of the spectrometer. Differences in target material as well as in target thickness were taken into account.

In the case of tridents, the contributions for both space-like and time-like virtual photons [Eqs. (25) and (42) in Ref. 24] were calculated. Since these were similar in magnitude for this experiment, the interference between the two (which can be of either sign) may be significant, but unfortunately no expression is given for this in Ref. 24. The result without interference terms is, however, in reasonable agreement with the experiment of Camac[25] within experimental errors of order 30% (i.e., it agrees with the expression of Bhabha[26] given by Rossi[23] when the constant K_2 is set equal to 1.35. The Camac result at 230 ± 20 MeV at 0.80 of the incident energy is $K_2=1.6\pm 0.2$). Measurements of the net pair-plus-trident background made using incident electrons and detecting positrons in the present geometry are shown in Fig. 3 along with the calculated results. The agreement within statistical errors is satisfactory after the data points have been shifted by 0.9% along the horizontal positron-momentum axis to take into account absolute differences in the spectrometer and deviation system momentum determinations. (A shift of 1.12 ± 0.08% found with incident positrons is discussed in detail later. The reproducibility of this shift is a measure of the reversibility of the magnet systems, while the shift itself is indicative of the absolute-energy uncertainties.)

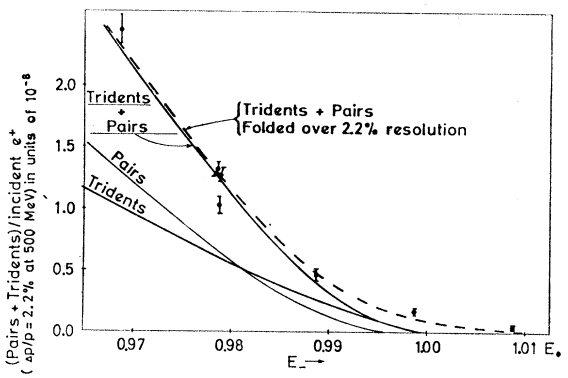

FIG. 3. Pair and trident backgrounds at 500 MeV. The data, shown with statistical errors, were taken with 0.0048 radiation lengths of aluminum plus 0.0072 radiation lengths of CH_2. The data have been shifted by 0.9% along the horizontal positron momentum axis to take into account absolute differences in the spectrometer and deviation-system momentum determinations.

The error in making the pair-production correction was taken to be 10% of the correction for the aluminum and polyethylene targets and 20% of the correction for bismuth. The larger uncertainty in the case of bismuth results from the failure of the Born approximation for high-Z elements.[23] The error assigned for Compton scattering is 20% of the correction at all points. The error assigned for trident production is 30% of the calculated correction due to neglecting the interference term. The sum of the corrections for annihilation followed by pair production and by Compton scattering was less than 2% for bismuth and less than 1% for the aluminum and polyethylene targets. These effects have

[22] In calculations involving the Bethe-Heitler formula we have used the program described by R. A. Alvarez, Jr., Hansen Laboratory Report No. HEPL-228, Stanford, California, 1961 (unpublished). This program is based on formulas found in the article of H. W. Koch and J. W. Motz, Rev. Mod. Phys. 31, 920 (1959) and is expected to be accurate to 2 or 3%.

[23] B. Rossi, *High Energy Particles* (Prentice-Hall, Inc., Englewood Cliffs, New Jersey, 1952), Chap. 2.

[24] T. Murota, A. Ueda, and H. Tanaka, Progr. Theoret. Phys. (Kyoto) 16, 482 (1956).

[25] M. Camac, Phys. Rev. 88, 745 (1952).

[26] H. Bhabha, Proc. Roy. Soc. (London) A152, 559 (1935).

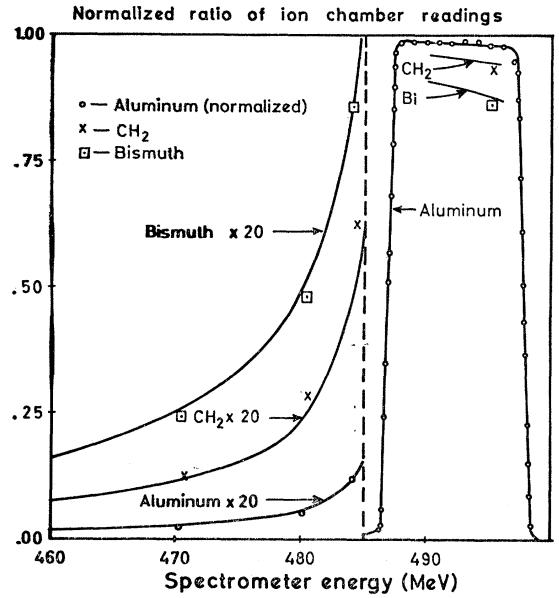

FIG. 4. Bremsstrahlung spectra obtained with aluminum, bismuth, and 3-mm polyethylene targets and with incident electrons at 500 MeV/c. The theoretical curves were obtained by folding together the Bethe-Heitler formula and the experimental momentum resolution. The difference in the peak height with and without material in the beam provides a rough estimate of the maximum bremsstrahlung loss. The data have been shifted slightly to compensate for ionization losses in the different targets.

been included in the pair-production and Compton-scattering corrections given in the tables.[27]

The corrections given for the losses due to bremsstrahlung in the target (δ_{TB}) were calculated by folding together the Bethe-Heitler formula and the experimental energy resolution. For these calculations, the Bethe-Heitler formula was multiplied by a "cutoff" function, $[1-e^{-4k^2}]$, which became effective for photons with energy $k \lesssim 0.5$ MeV. Check calculations using different cutoffs showed that the results were independent of the cutoff chosen over a reasonable range. The bismuth data again provided a test of our ability to make this correction, and the effect could be separated from multiple scattering and the various backgrounds by the fact that it decreased with decreasing p_-.

The numerical uncertainty in the calculation for target bremsstrahlung was about 3%, while there was an uncertainty of about 2% in the Bethe-Heitler formula itself.[22] As in the case of the other important corrections, an experimental test was possible. The bremsstrahlung spectra obtained with the aluminum, bismuth, and 3-mm polyethylene targets at 500 MeV are shown in Fig. 4 with the prediction derived from the Bethe-Heitler formula. The experimental results agree with these predictions to within about 5%. We assigned errors (ϵ_{TB}) of 5% of the bremsstrahlung correction and have not distinguished between relative and absolute uncertainties.

A π^- meson background was calculated to contribute $\lesssim 0.1\%$ to the observed counts in the worst case, because of the relative sizes of the cross sections.[28] No correction was made for this effect.

The energy of the incident particles was determined by both the spectrometer and the deviation magnets. One intercalibration was made with positrons incident and with the spectrometer detecting the recoil electrons, while the other was obtained with both systems set for electrons. The two methods gave the same answer to within 0.2%, thus indicating that the deviation magnet was reversible to this accuracy. This check was necessary because the floating-wire calibrations of the two magnet systems were made with the fields set for electrons. The calibrations were believed to be accurate to 0.2 or 0.3% and absolute agreement on this level was expected. The ratio of the energy given by the deviation magnet to that given by the spectrometer was 1.0060±0.0010 at 200 MeV and 1.0112±0.0008 at 500 MeV. The two calibrations were thus inconsistent

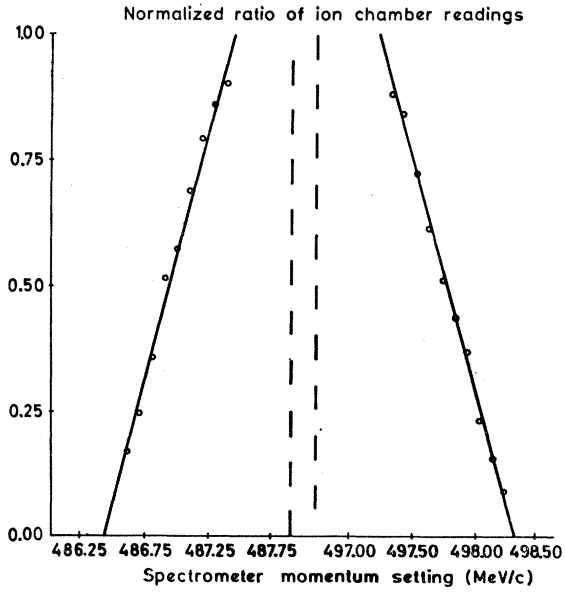

FIG. 5. Momentum acceptance of the spectrometer at 500 MeV/c. This figure shows the fast-rising portions of the curve obtained with aluminum in Fig. 4, with an expanded horizontal scale. The figure also shows the straight-line fit to the data used in measuring the slit width.

[27] As the tables indicate, the pair-plus-trident background increases rapidly as p_- decreases, and like multiple scattering, it is one of the factors limiting the range of p_- over which a high-precision experiment can be performed. Unlike multiple scattering and Compton scattering, the pair and trident corrections also increase with the incident positron momentum, and they would probably be the dominant errors in an experiment at very high energies. The pair and trident backgrounds can be controlled by using thin, low-Z targets, and they can be measured quite accurately by using incident electrons and by detecting the pair- and trident-produced positrons as was done in obtaining Fig. 3. Since the calculated corrections were small (~1%) at our data points, and since they were in good agreement with experimental tests such as that shown in Fig. 3, we have not felt it necessary to measure the backgrounds directly at every point.

[28] K. M. Watson, J. C. Keck, A. V. Tollestrup, and R. L. Walker, Phys. Rev. **101**, 1159 (1956).

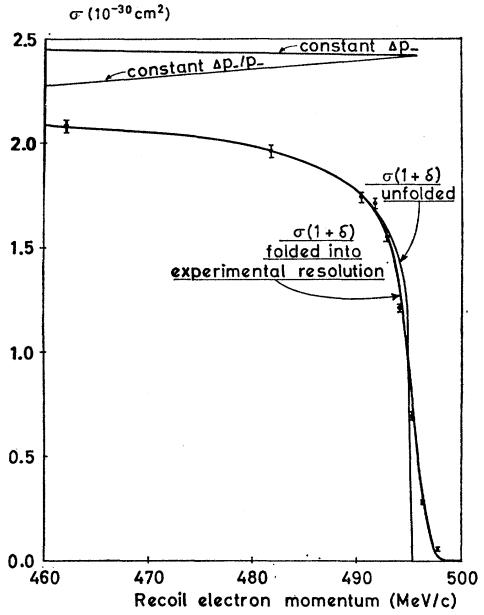

FIG. 6. High-resolution electron spectrum from positron-electron scattering at 500 MeV. The theoretical curves are for the uncorrected Bhabha cross section assuming constant Δp_-, the uncorrected Bhabha cross section assuming constant $\Delta p_-/p_-$, the Bhabha cross section for constant $\Delta p_-/p_-$ with radiative corrections of the form $(1+\delta)$, and the radiatively corrected cross section for constant $\Delta p_-/p_-$ folded over the finite momentum resolution. The data have been shifted along the horizontal p_- axis to obtain the best fit to the theory. The vertical coordinate has been renormalized by dividing the experimental cross sections at each point by the constant 1.024. The ± 0.17 MeV/c relative uncertainty in the location of the points on the spectrum is indicated by the width of the error bars. Other systematic errors which affect the shape of the spectrum have been combined with the statistical errors and are included in the height of the error bars.

both in value and in slope within the expected accuracy. We defined the energy to be the mean and assigned errors which included both measurements. The final energies were (200.2 ± 0.6) MeV and (495.7 ± 2.7) MeV The ratio of the energies was taken to be 2.476 ± 0.006, leading to symmetrical relative energy errors of ± 0.17 MeV at each point.

The spectrometer slit width was measured with an incident electron beam by recording the ratio of the readings obtained with the spectrometer ion chamber to those obtained with the beam ion chamber as a function of energy. The measurements at the two energies were made both by varying the deviation setting while keeping the spectrometer fixed, and by varying the spectrometer with the deviation field fixed. Typical results are shown in Figs. 4 and 5. These data were obtained at 500 MeV by varying the spectrometer field; and they are compared with the predicted curve for a roughly trapezoidal incident spectrum 0.55% wide at half-height, a uniform spectrometer response of 2.20%, and a radiative tail resulting from the beam passing through the aluminum and hydrogen of the beam monitor. The shape of the incident spectrum was due both to the size of the beam spot (3 mm×4 mm) and to the fact that the energy slits of the deviation system were not exactly at a "horizontal focus."

The precision of the spectrometer acceptance measurement depended on the stability of the magnetic fields and on the knowledge of the shape of the magnet calibration curve. The integration time for each point was long enough (~1 min) to provide a good average of the short-term fluctuations in the magnet regulation and yet short enough to minimize drifts during the total time required for the width measurement. Since the material in the beam was very thin, the full width at half-height could be taken as a direct measure of the momentum acceptance with negligible error. The half-height points were determined by fitting the data on the fast rising portions of the spectrum with a straight line, using the method of least squares. The errors in this procedure suggested that the individual measurements would be reproducible to about 0.3% if no shifts in energy occurred. A comparison of 5 measurements made at 500 MeV by varying the spectrometer showed that the standard deviation for a single measurement was about 0.6% thus indicating that significant drifts had occurred. Since the fluctuations were expected to be random, the measurements for a given set of conditions were averaged with equal weighting, and the error was taken to be the larger of 0.3% and the error calculated from the fluctuations. The values for the dispersion obtained by varying the spectrometer field were (0.3123 ± 0.0018)%/cm at 200 MeV and (0.3117 ± 0.0012)%/cm at 500 MeV. The results found by varying the deviation field were (0.3102 ± 0.0059)%/cm

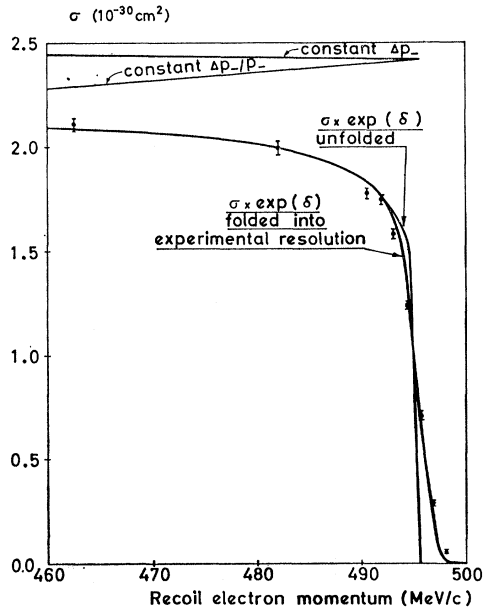

FIG. 7. High-resolution spectrum replotted for radiative corrections of the form e^{δ}. As in Fig. 6, the data have been shifted along p_- and have been normalized, in this case, by dividing each point by 1.010.

TABLE II. High-resolution spectrum at 500 MeV. The data were taken with $p_+=495.7$ MeV/c, $\Delta p_+/p_+=0.5\%$, $\Delta p_-/p_-=0.4710\%$, and a 15-mm×15-mm collimator. The targets listed in column 1 are described in detail in Sec. II. Column 2 gives $(p_--p_+)p/_+$ in percent after a small correction has been made for ionization in the target. Column 3 gives $d\sigma_0$, the cross section obtained with $\Delta p_-/p_-$ given above and corrected only for counting rate losses. The error in making the counting rate correction appears in column 4, pair-production corrections and errors in columns 5 and 6, trident corrections and errors in columns 7 and 8, Compton-scattering corrections and errors in columns 9 and 10, and target bremsstrahlung corrections and errors in columns 11 and 12. Additional relative corrections and errors are summarized in columns 13 and 14. These include: ±1.02% for $\Delta p_-/p_-$; ±0.21% for the beam monitors; an energy correction of less than 0.1 %due to ionization before scattering; a relative energy error of ±0.17 MeV; corrections and errors of (−0.19±0.03)% for bremsstrahlung in the counters; the small relative errors in target thickness; and a correction for annihilation in the target of less than 0.05%. The multiple-scattering correction was negligible at all points and is also included in columns 13 and 14. The relative uncertainty of ±0.17 MeV/c in the setting on the spectrum is indicated by the width of the vertical error bars in Fig. 6 where the high-resolution data are compared with theory. The net correction $(1+\delta_{\text{net}})=\pi_i(1+\delta_i)$, is given in column 15 and the final corrected cross section in column 16. Columns 17 and 18 give the statistical error derived from the number of counts taken and the relative systematic error computed by combining the various systematic errors quadratically. Additional absolute errors were bremsstrahlung in the counters, ±0.10% beam monitors, ±0.34%; energy, ±0.55%; and target thickness of ±0.4% for aluminum and ±0.3% for the other targets. The absolute errors were combined quadratically with the relative systematic errors to obtain the absolute systematic errors shown in column 19.

1	2	3	4	5	6	7	8	9	10	11	12	13	14	15	16	17	18	19
Target	$(p_--p_+)/p_+$ (% of p_+)	$d\sigma_0$ (10^{-29} cm^2)	ϵ_R	δ_{pp}	ϵ_{pp}	δ_{tri}	ϵ_{tri}	$\delta_{Compton}$	$\epsilon_{Compton}$	δ_{TB}	ϵ_{TB}	δ_{misc}	ϵ_{misc}	δ_{net}	$d\sigma_F$ (10^{-29} cm^2)	ϵ_{stat}	ϵ_{sys} Relative	ϵ_{sys} Absolute
3-mm CH_2	+0.91	<0.0001	±0.00	−0.00	±0.00	−0.00	±0.00	−0.00	±0.00	+6.95	±0.33	+0.35	±1.12	+7.30	<0.0001	···	±1.10	±1.37
3-mm CH_2	+0.41	0.0050	±0.00	−0.00	±0.00	−0.00	±0.00	−0.00	±0.00	+6.78	±0.32	+0.35	±1.12	+7.15	0.0054	±11	±1.10	±1.37
3-mm CH_2	+0.15	0.0270	±0.03	−0.00	±0.00	−0.00	±0.00	−0.03	±0.01	+6.66	±0.31	+0.35	±1.12	+7.00	0.0289	±3.5	±1.09	±1.36
3-mm CH_2	−0.08	0.0669	±0.10	−0.00	±0.00	−0.00	±0.00	−0.07	±0.02	+6.55	±0.30	+0.35	±1.12	+6.85	0.0715	±1.6	±1.09	±1.36
3-mm CH_2	−0.35	0.1178	±0.14	−0.12	±0.01	−0.05	±0.01	−0.12	±0.03	+6.38	±0.30	+0.35	±1.12	+6.45	0.1254	±1.2	±1.09	±1.36
3-mm CH_2	−0.60	0.1511	±0.13	−0.23	±0.02	−0.10	±0.03	−0.16	±0.04	+6.21	±0.29	+0.35	±1.12	+6.08	0.1602	±1.1	±1.09	±1.36
3-mm CH_2	−0.84	0.1673	±0.14	−0.34	±0.03	−0.15	±0.04	−0.22	±0.04	+5.93	±0.28	+0.35	±1.12	+5.57	0.1767	±1.0	±1.09	±1.36
3-mm CH_2	−1.11	0.1716	±0.18	−0.40	±0.04	−0.18	±0.05	−0.26	±0.05	+5.84	±0.28	+0.35	±1.12	+4.73	0.1798	±1.0	±1.10	±1.37
3-mm CH_2	−2.83	0.1973	±0.22	−1.06	±0.11	−0.50	±0.15	−0.70	±0.14	+4.76	±0.23	+0.35	±1.12	+2.82	0.2029	±1.0	±1.10	±1.37
Aluminum	−2.95	0.1984	±0.00	−0.44	±0.04	−1.10	±0.33	−0.18	±0.04	+1.11	±0.06	+0.39	±1.14	−0.22	0.1979	±2.5	±1.12	±1.39
Aluminum	−6.96	0.2005	±0.00	−1.36	±0.14	−2.82	±0.85	−0.26	±0.05	+0.92	±0.05	+0.39	±1.14	−3.14	0.1942	±5.2	±1.37	±1.62
3-mm CH_2	−6.84	0.2161	±0.26	−2.72	±0.27	−1.36	±0.41	−0.97	±0.20	+3.84	±0.19	+0.51	±1.12	+0.77	0.2144	±0.9	±1.18	±1.44

TABLE III. Low-resolution spectrum at 500 MeV. The data were taken with $p_-=495.7$ MeV/c, $\Delta p_+/p_+=0.5\%$, $\Delta p_-/p_-=2.203\%$, and a 7-mm×7-mm collimator. The notation is the same as in Table II, and the corrections and errors not shown explicitly are similar except that the relative uncertainty in $\Delta p_-/p_-$ is $=0.40\%$. The ± 0.17 MeV/c uncertainty in the setting on the recoil-electron spectrum is again indicated by the width of the vertical error bars in Fig. 8 where the low-resolution data at 500 MeV are plotted.

1	2	3	4	5	6	7	8	9	10	11	12	13	14	15	16	17	18	19
Target	$(p_- - p_+)/p_+$ (% of p_+)	$d\sigma_0$ (10^{-29} cm^2)	ϵ_R	$\delta_{p\gamma}$	ϵ_{pp}	δ_{tri}	ϵ_{tri}	$\delta_{Compton}$	$\epsilon_{Compton}$	δ_{TB}	ϵ_{TB}	δ_{misc}	ϵ_{misc}	δ_{net}	$d\sigma_F$ (10^{-29} cm^2)	ϵ_{stat}	ϵ_{sys} Relative	ϵ_{sys} Absolute
3-mm CH_2	+2.21	<0.0005	±0.00	−0.00	±0.00	−0.00	±0.00	−0.00	±0.00	+7.12	±0.33	+0.35	±0.60	+7.47	<0.0005	···	±0.68	±1.06
Bismuth	+2.11	<0.0014	±0.00	−0.00	±0.00	−0.00	±0.00	−0.00	±0.00	+15.9	±0.70	+0.39	±0.62	+16.3	<0.0016	···	±0.88	±1.20
Aluminum	+2.08	<0.0030	±0.00	−0.00	±0.00	−0.00	±0.00	−0.00	±0.00	+1.78	±0.09	+0.39	±0.61	+2.17	<0.0031	···	±0.62	±1.06
Aluminum	+1.07	0.0222	±0.00	−0.00	±0.00	−0.00	±0.00	−0.00	±0.00	+1.78	±0.09	+0.39	±0.64	+2.17	0.0227	±42	±0.65	±1.07
3-mm CH_2	+1.20	0.0085	±0.00	−0.00	±0.00	−0.00	±0.00	−0.00	±0.00	+7.12	±0.33	+0.35	±0.60	+7.49	0.0091	±23	±0.69	±1.06
Bismuth	+1.10	0.0174	±0.00	−0.00	±0.00	−0.00	±0.00	−0.00	±0.00	+15.9	±0.70	+0.39	±0.59	+16.3	0.0202	±26	±0.92	±1.14
Bismuth	+0.09	0.3271	±0.00	−0.00	±0.00	−0.00	±0.00	−0.00	±0.00	+15.5	±0.70	+0.39	±0.57	+15.9	0.3791	±5.3	±0.91	±1.22
3-mm CH_2	+0.17	0.2888	±0.00	−0.00	±0.00	−0.00	±0.00	−0.00	±0.00	+6.72	±0.32	+0.35	±0.57	+7.09	0.3092	±3.4	±0.66	±1.04
Aluminum	+0.06	0.3784	±0.00	−0.00	±0.00	−0.00	±0.00	−0.00	±0.00	+1.50	±0.07	+0.39	±0.59	+1.89	0.3856	±7.9	±0.60	±1.05
Aluminum	−0.97	0.7193	±0.00	−0.12	±0.01	−0.20	±0.06	−0.00	±0.00	+1.38	±0.07	+0.39	±0.58	+1.45	0.7297	±5.8	±0.60	±1.05
3-mm CH_2	−0.84	0.6477	±0.00	−0.40	±0.04	−0.17	±0.05	−0.25	±0.05	+6.04	±0.28	+0.35	±0.61	+5.48	0.6832	±1.9	±0.67	±1.05
Bismuth	−0.94	0.6625	±0.00	−2.49	±0.50	−1.13	±0.34	−0.72	±0.14	+14.1	±0.61	+0.39	±0.55	+10.9	0.7278	±2.3	±1.01	±1.29
Bismuth	−1.91	0.8728	±0.00	−6.81	±1.36	−2.52	±0.75	−1.07	±0.22	+11.6	±0.52	+0.39	±0.55	+1.12	0.8812	±2.2	±1.72	±1.89
3-mm CH_2	−1.83	0.8454	±0.01	−0.52	±0.05	−0.31	±0.09	−0.58	±0.12	+5.24	±0.25	+0.35	±0.56	+4.17	0.8806	±1.8	±0.61	±1.05
Aluminum	−1.95	0.9252	±0.02	−0.22	±0.02	−0.77	±0.23	−0.14	±0.03	+1.41	±0.07	+0.39	±0.58	+0.67	0.9314	±3.7	±0.62	±1.06
Aluminum	−2.99	0.9319	±0.02	−0.44	±0.04	−1.10	±0.33	−0.18	±0.04	+1.10	±0.05	+0.39	±0.59	−0.23	0.9297	±1.8	±0.67	±1.08
3-mm CH_2	−2.86	0.9086	±0.18	−1.14	±0.11	−0.54	±0.16	−0.53	±1.10	+4.75	±0.23	+0.35	±0.55	+2.83	0.9342	±1.1	±0.64	±1.03
Bismuth	−3.93	1.0600	±0.07	−17.51	±3.50	−4.55	±1.36	−1.32	±0.26	+10.7	±0.46	+0.39	±0.57	−13.90	0.9185	±2.1	±3.8	±4.0
3-mm CH_2	−3.84	0.9573	±0.22	−1.44	±0.14	−0.68	±0.20	−0.79	±0.16	+4.38	±0.21	+0.35	±0.55	+1.75	0.9737	±1.3	±0.65	±1.04
Aluminum	−3.96	0.9057	±0.02	−0.66	±0.07	−1.58	±0.47	−0.21	±0.04	+1.06	±0.05	+0.39	±0.57	−1.00	0.8966	±3.9	±0.74	±1.13
Aluminum	−6.67	0.9817	±0.02	−1.22	±0.12	−2.68	±0.80	−0.25	±0.05	+0.94	±0.05	+0.39	±0.57	−2.82	0.9541	±3.3	±0.99	±1.30
3-mm CH_2	−6.55	0.9942	±0.18	−2.69	±0.27	−1.32	±0.40	−0.98	±0.20	+3.89	±0.19	+0.35	±0.55	−0.83	0.9859	±1.3	±0.72	±1.09
Bismuth	−6.65	1.3080	±0.09	−32.0	±6.4	−7.45	±2.23	−1.34	±0.26	+8.87	±0.15	+0.39	±0.56	−33.6	0.8964	±1.9	±6.9	±6.3
1-mm CH_2	−6.63	0.9855	±0.13	−1.75	±0.18	−1.89	±0.57	−0.58	±0.12	+1.93	±0.09	+0.38	±0.55	−1.91	0.9664	±1.6	±0.80	±1.14

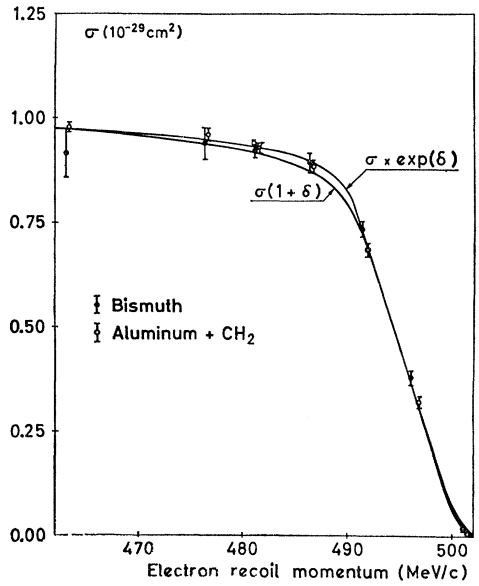

FIG. 8. Low-resolution spectrum at 500 MeV/c. The unnormalized data with relative errors are shown along with the theoretical curves for $(1+\delta)$ and e^{δ}. The aluminum and polyethylene data have been combined for clarity, but the bismuth check points are shown separately. The ± 0.17 MeV/c relative uncertainty in the energy is shown by the width of the error bars.

at 200 MeV and $(0.3137\pm 0.0013)\%$/cm at 500 MeV. Floating-wire measurements gave $(0.316\pm 0.009)\%$/cm while the value calculated from the spectrometer parameters was about 0.326%/cm.

The calculated dispersion for this spectrometer[20] depends upon the "n value" of the field, which in turn depends upon the saturation characteristics of the three magnets. From the measured variation of n with the field setting,[20] we estimated that the ratio of the values at 500 and 200 MeV should be 1.012 ± 0.006. A weighted average of the dispersion measurements gave $(0.3123\pm 0.0006)/(0.3114\pm 0.0009)=(1.0029\pm 0.0032)$ while the average with equal weighting was $(0.3122\pm 0.0010)/(0.3112\pm 0.0026)=(1.0032\pm 0.0089)$. This ratio for the spectrometer separately was (0.9981 ± 0.0005) and for the deviation system (1.011 ± 0.019). Within the errors assigned from the fluctuations, the present ratio measurements were self-consistent but somewhat lower than the predictions from the measured n values.

In comparing the experiment with theory, we combined the directly measured values with equal weighting to obtain for our (7.054 ± 0.004)-cm slit width:

$$\Delta p_-/p_-(500\text{ MeV})=2.203\%,$$

and

$$\Delta p_-/p_-(200\text{ MeV})=2.195\%.$$

We assigned relative errors of $\pm 0.40\%$ at each energy, leading to a $\pm 0.60\%$ uncertainty in the ratio, and we assigned additional absolute errors of $\pm 0.40\%$, resulting in absolute errors of $\pm 0.60\%$. Within these errors all of the data on $\Delta p_-/p_-$ were consistent, including the result obtained from the variation of n.

The value of $\Delta p_-/p_-$ for the high-resolution spectrum was not measured directly; thus these data were normalized to the absolute results of the low-resolution spectrum and "data" points. The normalization was done at points taken with the same target and momentum settings so that systematic errors in the normalization were negligible compared to the statistical error of $\pm 0.94\%$. This error was combined quadratically with the error in the dispersion to obtain the absolute error in $\Delta p_-/p_-$ for the high-resolution data.

Since the measurements of $\Delta p_-/p_-$ and $p_-\approx p_+$ were not independent, it was important to consider to what extent the errors in these quantities were correlated. To test this, we calculated the ratio of the cross sections in terms of the spectrometer and deviation measurements.

$$d\sigma_{\text{spec}}/d\sigma_{\text{dev}}\approx\frac{1}{E_{\text{spec}}}\left(\frac{\Delta p_-}{p_-}\right)_{\text{spec}}\Big/\frac{1}{E_{\text{dev}}}\left(\frac{\Delta p_-}{p_-}\right)_{\text{dev}}$$

$$\approx\frac{(1.0112\pm 0.0008)(0.3117\pm 0.0012)}{0.3137\pm 0.0013}$$

$$\approx 1.005\pm 0.006 \quad \text{at} \quad 500\text{ MeV} \tag{12}$$

$$\approx\frac{(1.0060\pm 0.0010)(0.3123\pm 0.0018)}{0.3102\pm 0.0059}$$

$$\approx 1.013\pm 0.020 \quad \text{at} \quad 200\text{ MeV}. \tag{13}$$

Because of the large random error in the deviation measurement at 200 MeV, the test at this energy was not very informative. The test at 500 MeV suggested,

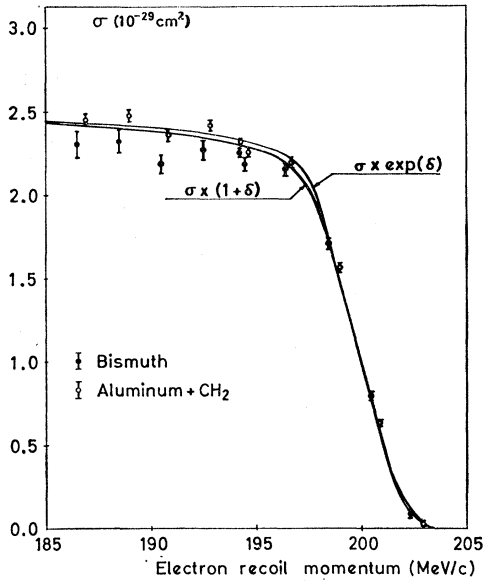

FIG. 9. Low-resolution spectrum at 200 MeV/c. The ± 0.09 MeV/c uncertainty in the relative position of each point on the spectrum is indicated by the width of the error bars, while the relative error is indicated by the height.

TABLE IV. Low-resolution spectrum at 200 MeV. The data in this table were taken with $p_+=200.2$ MeV/c, $\Delta p_+/p_+=1.0\%$, $\Delta p_-/p_-=2.195\%$, and a 7-mm×7-mm collimator. Columns 5 and 6 give the multiple-scattering correction and error. The miscellaneous corrections and errors included in columns 15 and 16 are +0.12% due to beam monitors; (+0.32±0.06)% due to bremsstrahlung in the counters; and the relative errors in target thickness given in Sec. II. The absolute systematic errors were estimated by combining quadratically the relative systematic errors and errors of ±0.16% due to bremsstrahlung in the counters; ±0.34% due to beam monitors; ±0.30% uncertainties in the energy; and the absolute errors in target thickness given in the text. An uncertainty of ±0.09 MeV/c in the spectrum setting is shown by the width of the vertical error bars in Fig. 9.

1	2	3	4	5	6	7	8	9	10	11	12	13	14	15	16	17	18	19	20	21
Target	$(p_--p_+)/p_+$ (% of p_+)	$d\sigma_0$ (10^{-29} cm^2)	ϵ_R	δ_{ms}	ϵ_{ms}	δ_{pp}	ϵ_{pp}	δ_{tri}	ϵ_{tri}	$\delta_{Compton}$	$\epsilon_{Compton}$	δ_{TB}	ϵ_{TB}	δ_{misc}	ϵ_{misc}	δ_{net}	$d\sigma_F$ (10^{-29} cm^2)	ϵ_{stat}	ϵ_{sys} Relative	ϵ_{sys} Absolute
3-mm CH_2	+2.29	0.0004	±0.00	+0.00	±0.00	−0.00	±0.00	−0.00	±0.00	−0.00	±0.00	+6.72	±0.32	+0.25	±0.51	+6.97	0.004	···	±0.61	±0.83
3-mm CH_2	+1.32	0.0232	±0.00	+0.00	±0.00	−0.00	±0.00	−0.00	±0.00	−0.00	±0.00	+6.72	±0.32	+0.25	±0.51	+6.97	0.0248	±13	±0.61	±0.83
Bismuth	+1.08	0.0797	±0.00	+0.00	±0.00	−0.00	±0.00	−0.00	±0.00	−0.00	±0.00	+15.9	±0.68	+0.35	±0.51	+16.3	0.0927	±12	±0.85	±1.04
Aluminum	+1.02	0.1294	±0.00	+0.00	±0.00	−0.00	±0.00	−0.00	±0.00	−0.00	±0.00	+1.72	±0.09	+0.36	±0.54	+2.08	0.1321	±15	±0.55	±0.83
Aluminum	+0.01	0.8131	±0.00	+0.00	±0.00	−0.00	±0.00	−0.00	±0.00	−0.00	±0.00	+1.43	±0.07	+0.36	±0.54	+1.79	0.8276	±4.9	±0.51	±0.80
3-mm CH_2	+0.32	0.5907	±0.10	+0.00	±0.00	−0.00	±0.00	−0.00	±0.00	−0.04	±0.01	+6.02	±0.38	+0.25	±0.49	+6.24	0.6276	±1.8	±0.58	±0.81
Bismuth	+0.08	0.6844	±0.04	+0.00	±0.00	−0.00	±0.00	−0.00	±0.00	−0.23	±0.04	+15.00	±0.65	+0.35	±0.48	+15.17	0.7882	±2.5	±0.81	±0.99
Bismuth	−0.89	1.475	±0.09	+2.00	±0.20	−0.14	±0.03	−0.15	±0.05	−0.29	±0.06	+13.12	±0.58	+0.35	±0.48	+15.14	1.700	±1.7	±0.79	±0.97
3-mm CH_2	−0.65	1.520	±0.42	+0.10	±0.01	−0.00	±0.00	−0.00	±0.00	−0.08	±0.02	+5.76	±0.27	+0.25	±0.52	+6.05	1.612	±1.4	±0.71	±0.91
Aluminum	−0.95	1.861	±0.01	+0.00	±0.00	−0.00	±0.00	−0.00	±0.00	−0.00	±0.00	+1.33	±0.07	+0.36	±0.50	+1.69	1.892	±2.3	±0.51	±0.80
Aluminum	−1.97	2.216	±0.05	+0.03	±0.01	−0.03	±0.00	−0.12	±0.04	−0.07	±0.02	+1.11	±0.06	+0.36	±0.51	+1.28	2.244	±2.2	±0.52	±0.81
3-mm CH_2	−1.66	2.055	±0.12	+0.63	±0.06	−0.13	±0.01	−0.08	±0.02	−0.26	±0.05	+5.02	±0.24	+0.25	±0.62	+5.46	2.167	±1.5	±0.68	±0.89
Bismuth	−1.90	1.891	±0.14	+4.15	±0.42	−1.23	±0.24	−0.57	±0.17	−0.58	±0.12	+11.13	±0.50	+0.35	±0.47	+14.92	2.153	±1.5	±0.88	±1.04
Bismuth	−2.92	1.933	±0.14	+6.32	±0.63	−2.92	±0.58	−1.46	±0.44	−0.86	±0.17	+10.13	±0.45	+0.35	±0.47	+11.82	2.155	±1.4	±1.16	±1.30
3-mm CH_2	−2.68	2.121	±0.45	+1.65	±0.17	−0.33	±0.03	−0.18	±0.05	−0.39	±0.08	+3.30	±0.19	+0.25	±0.50	+4.34	2.212	±1.2	±0.70	±0.90
Aluminum	−2.98	2.286	±0.07	+0.08	±0.02	−0.08	±0.01	−0.26	±0.08	−0.10	±0.02	+1.01	±0.05	+0.30	±0.49	+1.01	2.309	±1.5	±0.52	±0.81
Aluminum	−3.90	2.336	±0.05	+0.11	±0.02	−0.16	±0.02	−0.49	±0.15	−0.12	±0.02	+0.93	±0.05	+0.36	±0.49	+0.61	2.351	±1.9	±0.52	±0.81
3-mm CH_2	−3.60	2.303	±0.28	+3.18	±0.32	−0.49	±0.05	−0.30	±0.09	−0.41	±0.09	+4.02	±0.19	+0.25	±0.49	+6.31	2.449	±1.2	±0.64	±0.90
Bismuth	−3.84	2.091	±0.14	+8.61	±0.86	−4.46	±0.90	−2.02	±0.60	−0.98	±0.20	+9.11	±0.42	+0.35	±0.49	+11.05	2.305	±1.8	±1.54	±1.64
Bismuth	−4.96	2.003	±0.11	+11.33	±1.13	−7.54	±1.50	−2.83	±0.33	−1.21	±0.24	+8.51	±0.39	+0.35	±0.51	+7.91	2.237	±1.8	±2.05	±2.10
3-mm CH_2	−4.62	2.225	±0.27	+5.53	±0.55	−0.64	±0.06	−0.34	±0.09	−0.56	±0.12	+3.74	±0.18	+0.25	±0.51	+8.14	2.407	±1.2	±0.81	±0.99
Aluminum	−4.93	2.338	±0.05	+0.17	±0.05	−0.20	±0.02	−0.61	±0.18	−0.14	±0.03	+0.89	±0.05	+0.36	±0.52	+0.47	2.349	±2.0	±0.55	±0.83
Aluminum	−5.87	2.443	±0.07	+1.60	±0.16	−0.27	±0.03	−0.81	±0.24	−0.15	±0.03	+0.79	±0.04	+0.36	±0.51	+1.52	2.480	±1.8	±0.59	±0.85
3-mm CH_2	−5.57	2.238	±0.40	+9.42	±0.84	−0.83	±0.08	−0.43	±0.12	−0.60	±0.12	+3.56	±0.17	+0.25	±0.49	+10.61	2.474	±1.1	±1.08	±1.22
Bismuth	−5.81	2.130	±0.22	+14.05	±1.40	−9.09	±1.80	−3.37	±1.01	−1.25	±0.25	+8.09	±0.37	+0.35	±0.48	+7.47	2.289	±1.7	±2.52	±2.58
Bismuth	−6.81	2.157	±0.14	+17.0	±1.70	−12.43	±2.48	−4.13	±1.24	−1.37	±0.27	+7.70	±0.36	+0.35	±0.48	+4.83	2.261	±1.7	±3.38	±3.44
3-mm CH_2	−6.57	2.166	±0.40	+11.8	±1.18	−0.96	±0.10	−0.55	±0.17	−0.73	±0.15	+3.39	±0.16	+0.25	±0.47	+13.42	2.458	±1.0	±1.32	±1.43
Aluminum	−6.07	2.275	±0.05	+2.45	±0.25	−0.29	±0.03	−0.86	±0.26	−0.16	±0.04	+3.47	±0.17	+0.36	±0.50	+5.00	2.389	±2.1	±0.66	±0.91

TABLE V. Data at 500 and 200 MeV. The 500-MeV data were taken with $p_+=495.7$ MeV/c, $\Delta p_+/p_+=0.5\%$, $\Delta p_-/p_-=2.203\%$, and a 5-mm×5-mm collimator. The 200-MeV data were taken with $p_+=200.2$ MeV/c, $\Delta p_+/p_+=1.0\%$, $\Delta p_-/p_-=2.195\%$, and a 8-mm×8-mm collimator. The differences in $\Delta p_+/p_+$ and in the collimator settings slightly alter the shape of the electron spectrum, but have negligible effect on the counting rate 3% down from p_-. A small spectrum correction was made to the data to obtain values exactly 3% down. This correction and the uncertainties in the spectrum setting, amounting to about ±0.05%, have been included in the miscellaneous corrections and errors of columns 15 and 16. Other miscellaneous and absolute contributions are as in Tables III and IV for the respective values of p_+.

1	2	3	4	5	6	7	8	9	10	11	12	13	14	15	16	17	18	19	20	21
Target	p_- corrected to −3% MeV	$d\sigma_0$ (10^{-29} cm^2)	ϵ_E	δ_{ms}	ϵ_{ms}	δ_{pp}	ϵ_{pp}	δ_{tri}	ϵ_{tri}	$\delta_{Compton}$	$\epsilon_{Compton}$	δ_{TB}	ϵ_{TB}	δ_{mise}	ϵ_{mise}	δ_{net}	$d\sigma_T$ (10^{-29} cm^2)	ϵ_{stat}	ϵ_{sys} Relative	ϵ_{sys} Absolute
Aluminum	480.90	0.9297	±0.08	0.00	±0.00	−0.44	±0.04	−1.10	±0.33	−0.18	±0.04	+1.10	±0.05	+0.41	±0.48	−0.21	0.9276	±1.34	±0.59	±1.04
1-mm CH_2	480.90	0.9219	±0.15	0.00	±0.00	−0.70	±0.07	−0.80	±0.24	−0.43	±0.08	+2.35	±0.12	+0.50	±0.46	+0.92	0.9302	±0.75	±0.55	±0.98
2-mm CH_2	480.90	0.9397	±0.26	0.00	±0.00	−0.88	±0.09	−0.60	±0.18	−0.54	±0.11	+3.41	±0.17	+0.58	±0.46	+1.94	0.9582	±0.72	±0.58	±0.99
3-mm CH_2	480.90	0.9139	±0.31	0.00	±0.00	−1.17	±0.12	−0.50	±0.15	−0.73	±0.14	+4.76	±0.23	+0.64	±0.46	+3.00	0.9415	±0.63	±0.62	±1.02
Bismuth	480.90	0.9714	±0.13	0.00	±0.00	−11.22	±2.24	−3.53	±1.06	−1.26	±0.25	+10.9	±0.48	+0.47	±0.46	−7.47	0.9005	±1.05	±2.55	±2.68
2-mm CH_2	480.90	0.9102	±0.28	0.00	±0.00	−0.88	±0.09	−0.60	±0.18	−0.57	±0.12	+3.41	±0.17	+0.59	±0.46	+1.94	0.9276	±0.73	±0.58	±0.99
Aluminum	194.20	2.283	±0.05	+0.08	±0.01	−0.11	±0.01	−0.35	±0.10	−0.10	±0.02	+1.01	±0.05	+0.44	±0.51	+0.97	2.306	±0.89	±0.48	±0.79
1-mm CH_2	194.20	2.253	±0.16	+0.42	±0.04	−0.18	±0.02	−0.23	±0.07	−0.24	±0.04	+2.14	±0.11	+0.64	±0.52	+2.57	2.311	±0.62	±0.52	±0.77
2-mm CH_2	194.20	2.241	±0.15	+1.25	±0.13	−0.25	±0.03	−0.19	±0.06	−0.30	±0.06	+3.14	±0.15	+0.80	±0.52	+4.53	2.343	±0.52	±0.55	±0.77
3-mm CH_2	194.20	2.187	±0.21	+1.60	±0.16	−0.36	±0.04	−0.16	±0.06	−0.41	±0.08	+4.38	±0.21	+1.00	±0.55	+6.17	2.322	±0.55	±0.62	±0.84
Bismuth	194.20	2.012	±0.09	+6.30	±0.63	−3.06	±0.61	−1.96	±0.45	−0.83	±0.17	+9.82	±0.45	+0.57	±0.53	+10.69	2.225	±0.70	±1.22	±1.32
3-mm CH_2	194.20	2.217	±0.21	+1.60	±0.16	−0.36	±0.04	−0.16	±0.06	−0.41	±0.08	+4.38	±0.21	+1.00	±0.52	+6.17	2.353	±0.69	±0.62	±0.84

however, that the correlation of the systematic errors in p_+ and $\Delta p_-/p_-$ was negative and that the net error derived by combining the separate errors quadratically was conservative.

IV. DISCUSSION

A most sensitive test of the radiative corrections was provided by the shape of the high-resolution spectrum at 500 MeV. In making this test the data were normalized to the theory and shifted along the horizontal (p_-) axis to obtain the best fit. In Figs. 6 and 7 these data are plotted along with the Bhabha cross section assuming constant Δp_-; the Bhabha cross section assuming constant $\Delta p_-/p_-$; the Bhabha cross section for constant $\Delta p_-/p_-$ with radiative corrections of the form $1+\delta$ (Fig. 6) and e^δ (Fig. 7); and the radiatively corrected cross section for constant $\Delta p_-/p_-$ folded over the experimental momentum resolution. Two figures are necessary since the normalization and shift required were slightly different for each type of radiative correction. The errors were obtained by combining quadratically those errors in Table II which would change the shape of the spectrum. The width of the error bar indicates the ±0.17 MeV/c relative uncertainty in the location of each point on the spectrum.

It is evident from the figures that the data agree very well with the predictions when a radiative correction of the form $1+\delta$ is used (χ^2 probability of 0.50) and that the agreement is less good with the form e^δ (χ^2 probability of 0.20). It should be emphasized again that complete radiative corrections for this experiment are not available[11]; the radiative corrections used are an extrapolation from the case $\Delta\theta_4 \ll \theta_4$ treated in Ref. 10. Thus it is possible that the agreement with the two forms may change.

The unnormalized spectra obtained at 500 and 200 MeV are shown, along with the data points, in Figs. 8 and 9. The data from the different polyethylene targets and the aluminum target have been combined in these figures. The data taken with the different targets agreed well, and there was no indication that unanticipated Z-dependent effects were present. The figures also show the theoretical curves for the two types of radiative corrections. The theoretical curves have been shifted to coincide at the fast-rising portion of the data. This procedure changes the ratio of experiment/theory at some points by as much as 0.5%, but the general features of the comparison are still represented correctly.

The most sensitive measure of the absolute value of the cross sections was given by the "data" points taken at $p_+-3\%$. The theoretical values used were

$$\sigma_{\text{theory}}(p_+=495.7\ \text{MeV}/c,\ p_-=0.9700p_+,\ \Delta p_-/p_- =2.203\%)=1.102\times10^{-29}\ \text{cm}^2,\quad \delta=-0.163, \tag{14}$$

$$\sigma_{\text{theory}}(p_+=200.2\ \text{MeV}/c,\ p_-=0.9700p_+,\ \Delta p_-/p_- =2.195\%)=2.724\times10^{-29}\ \text{cm}^2,\quad \delta=-0.155. \tag{15}$$

TABLE VI. Results of absolute measurements.

	$\sigma_{th}(1+\delta)$ (10^{-29} cm^2)	$\sigma_{th}e^{\delta}$ (10^{-29} cm^2)	σ_{expt} (10^{-29} cm^2)	$\sigma_{expt}/\sigma_{th}(1+\delta)$	$\sigma_{expt}/\sigma_{th}e^{\delta}$
500 MeV	0.9222	0.9363	0.9384	1.018±0.011	1.003±0.011
200 MeV	2.303	2.333	2.329	1.011±0.009	0.998±0.009
$\sigma_{500}/\sigma_{200}$	0.4004	0.4013	0.4031	1.007±0.009	1.005±0.009

For this "test of QED" the polyethylene and aluminum data from Table V were combined to reduce the statistical errors. The systematic error used was the statistically weighted average of the separate systematic errors. The final error was obtained by combining the statistical and systematic errors quadratically. Table VI gives the results of the *absolute* measurements. Relative errors are used in the row labeled "ratio," while *absolute* errors are given with the other experimental values.

As Table VI shows, the *absolute* values are in agreement with the theory if radiative corrections of the form e^{δ} are used, but in less good agreement with the theory if corrections of the form $1+\delta$ are used. While neither the recoil spectrum measurements [which favor $1+\delta$] nor the *absolute* values [which favor e^{δ}] is sufficiently precise to eliminate one form or the other, nevertheless, the over-all agreement with the radiatively corrected electrodynamic cross sections is excellent on the 1% level. If the radiative corrections are assumed to be precisely known, this experiment determines $1/K$ in Eq. (1) to about 0.6 F.

ACKNOWLEDGMENTS

This experiment would have been impossible without the cooperation and help of many people in the Linear Accelerator Laboratory. In particular, we would like to acknowledge the generous support of Professor A. Blanc-Lapierre. In addition, we also wish to thank Dr. B. Milman for his assistance, Dr. L. Burnod for adapting the Orsay positron beam to the conditions of this experiment, R. Tchapoutian for his participation in the data runs, and V. Round for suggestions on the construction of the thin ion chamber.

One of us (D. Y.) was supported by the National Science Foundation Postdoctoral Fellowship during the course of this work.